Title: Tracheal chambers as a key innovation for high frequency emission in bat echolocation.

Nicolas LM Brualla[1], Laura AB Wilson[2,3,4]*, Khizar Hayat[5,6], Michael Doube[1], Vuong Tan Tu[7,8], Thongchai Ngamprasertwong[9], Thanakul Wannaprasert[9], Daisuke Koyabu[1,10]*.

1. Department of Infectious Diseases and Public Health, Jockey Club College of Veterinary Medicine and Life Sciences, City University of Hong Kong, Hong Kong SAR, China

2. School of Archaeology and Anthropology, College of Arts and Social Sciences, The Australian National University, Acton, ACT 2601, Australia

3. School of Biological, Earth and Environmental Sciences, University of New South Wales, Kensington, NSW 2052, Australia

4. ARC Training Centre for Multiscale 3D Imaging, Modelling, and Manufacturing, Research School of Physics, The Australian National University, Acton, ACT 2601, Australia

5. Jockey Club College of Veterinary Medicine and Life Sciences, City University of Hong Kong, Hong Kong SAR, China

6. Department of Clinical Sciences, College of Veterinary Medicine, Cornell University, New York, 14850, USA

7. Institute of Ecology and Biological Resources, Vietnam Academy of Science and Technology, Hanoi, Vietnam

8. Graduate University of Science and Technology, Vietnam Academy of Science and Technology, Hanoi, Vietnam

9. Department of Biology, Faculty of Science, Chulalongkorn University, Bangkok, Thailand

10. Research and Development Center for Precision Medicine, University of Tsukuba, Tsukuba, Japan

Corresponding authors

*Laura A.B. Wilson: laura.wilson@anu.edu.au

*Daisuke Koyabu: dsk8evoluxion@gmail.com

ORCID iDs

NB: 0000-0003-1367-0778; LW: 0000-0002-3779-8277; KH: 0000-0002-0950-9351; MD: 0000-0002-8021-8127; VTT: 0000-0002-5915-865X; TN: 0000-0003-3146-1849; TW: 0000-0002-6695-1015; DK: 0000-0002-4087-7742

Abstract

Key innovations play a crucial role in driving biodiversity and facilitating evolutionary success by enabling organisms to adapt to various ecological niches through the diversification of phenotypic traits. These innovations have been observed in different vertebrate clades, such as mammals evolving hypsodonty to graze on contemporary grasses and bats with the evolution of echolocation, alongside wing acquisition. Recent studies have shed light on the overlooked morphological diversity of the larynx in bats, a key organ involved in echolocation capabilities. Tracheal chambers, found on the first rings of the trachea, are enigmatic components of the laryngeal complex whose origins and functions have yet to be fully elucidated. We hypothesised that these structures may show evolutionary convergence and represent a key innovation associated with laryngeal echolocation. The present study examines 50 bat species, their laryngeal cartilages and tracheal chambers. We explored relationships between body mass, sound frequencies, and chamber volumes, as we hypothesise that tracheal chambers may have facilitated laryngeal echolocation capabilities in bats. Ancestral state reconstructions were conducted to understand the evolution of tracheal chambers and laryngeal echolocation behaviours in bats. We conclude that tracheal chambers allow higher frequency sound production and were pivotal for the specialization of high-duty cycle echolocation during the evolution of bats emitting calls nasally, contributing to their ability to thrive in diverse environments. We suggest that tracheal chambers are key innovations that enhance laryngeal echolocation behaviours and the evolutionary success of bats.

Introduction

Through the diversification of phenotypic traits and functional adaptations, key innovations enable organisms to exploit novel ecological opportunities (Miller et al., 2023). Key innovations unlock species evolutionary success by triggering adaptative radiations. Previous studies have

illustrated such phenomena in different vertebrate clades. For example, several groups of herbivorous mammals acquired hypsodonty (modification of high crown tooth height) and shifted their diet to graze on more abrasive, contemporary grasses which enabled them to adapt to climatic fluctuations during the Miocene transitions (DeMiguel et al., 2014). Similarly, vertebral modifications of the cetacean axial skeleton were key innovations that allowed a great radiation of these mammals by colonisation of the open seas (Gillet et al., 2019).

Bats are another example of formidable morphological innovation and evolutionary success. Through colonisation of diverse ecological niches, bats thrived and speciated, and are now the second most speciose mammalian group with 25% of all mammalian species (Simmons and Cirranello, 2020). In this context, the acquisition of wings for self-powered flight and the production of high frequency calls for echolocation are considered potential key innovations behind the ecological diversification and evolutionary success of bats (Fenton, 2013). Evolutionary modifications of the larynx might have allowed bats to produce and control those high frequency pulses critical for echolocation behaviour (laryngeal echolocation). Therefore, the larynx could be directly involved in the evolutionary success of bats. Still, little is known about the laryngeal morphology in this clade. Recent efforts have revealed the overlooked diversity and peculiarity of chiropteran larynges, but many aspects of the bat larynx require further investigation to understand how laryngeal function enables the production and coordination of high frequency pulses (Brualla et al., 2023, 2024).

Tracheal chambers are hollow cartilaginous spheres located on the first rings of the trachea, whose origin and function remain unclear (Figure 1). In bats, these chambers are found in all representatives of the monophyletic clade consisting of rhinolophids (Rhinolophidae), hipposiderids (Hipposideridae), and rhinonycterids (Rhinonycteridae) distributed in Eurasia, and in the distantly related nycterids (Nycteridae). Tracheal chambers are anatomically distinct from the laryngeal ventricles found in most mammals between the vestibular and vocal folds (Harrison,

1995). Developmental observation in *Rhinolophus* reported that the chambers are mineralized outgrowths of the cricoid cartilage (Nojiri et al., 2024). Rhinolophids (Rhinolophidae) and Hipposiderids (Hipposideridae) possess two to four cartilaginous swellings along their trachea (Robin, 1881; Schneider, 1964; Denny, 1976; Brualla et al., 2024). Generally, rhinolophids have larger chambers than hipposiderids relative to body size (Denny, 1976; Brualla et al., 2024). Nycterids (Nycteridae), the third family possessing tracheal chambers, have only a pair of large lateral chambers (Elias, 1907; Denny, 1976; Griffiths, 1994; Nojiri et al., 2024). However, the functional significance of these variations in number of chambers and chamber size remain largely unclear. Tracheal chambers were often functionally compared to the laryngeal air sacs present in the Siamang gibbon (*Symphalangus syndactylus*), with the distinction that bat chambers are made of an unusual mineralized cartilaginous structure (Elias, 1907; Hartley and Suthers, 1988). These chambers could be implicated in regulating laryngeal echolocation. Dorsal chambers may contribute to vocal specializations by enhancing sound amplitude through the reflection of emitted sound within the trachea (Au and Suthers, 2014; Ma et al., 2016). On the other hand, lateral chambers might serve to filter fundamental frequencies, enhancing the signal's frequency at the second harmonic (Ma et al., 2016). Tracheal chambers have also been suggested to potentially support nasal sound emission in bats (Denny, 1976).

Bats with chambers include most constant-frequency high-duty cycle (CF HDC) specialists (rhinolophids, hipposiderids, and rhinonycterids) and most nasal emitting species (excluding Megadermatidae, Rhinopomatidae and Phyllostomidae species) (Harrison, 1995; Au and Suthers, 2014; Brualla et al., 2024). This distribution across bat phylogeny implies unexplored evolutionary convergence among nasal emitters. Surprisingly, no investigations have examined the relationship between echolocation types and the morphology of the chambers, particularly regarding the evolutionary convergence associated with the acquisition of these chambers. In addition, we

suggest that acquisition of the tracheal chambers might have enable bats to reach new ecological niches.

For the first time, we present qualitative and quantitative comparisons of tracheal chambers in a wide range of bat species within a rigorous phylogenetic framework to investigate the potential role of chambers in laryngeal echolocation. We apply computational evolutionary models to infer the evolutionary history of tracheal chambers in bats and test whether these chambers may have facilitated echolocation capabilities. Our results show that tracheal chambers allow higher frequency pulses in nasal emitting bats and highlight that these chambers are a key innovation that allowed bats to exploit new ecological opportunities.

Results

Morphological comparisons

Anatomy

All larynges reconstructed in this study were consistent with previous descriptions of larynges from similar bat clades, allowing distinction between the outgroup and Pteropodidae morphology from the Rhinolophoidea larynges (Brualla et al., 2024). The extreme development of muscular wings and median crest on the cricoid cartilage, as well as the reduction of the cricoid arch were visible on the larynx of Rhinolophidae, Hipposideridae, and Rhinonycteridae species, and absent from Pteropodidae larynges (Figure 1). Three-dimensional reconstructions of *Nycteris tragata* larynges revealed novel anatomical features. The chambers of *Nycteris tragata* are positioned caudally to the cricoid cartilage, located on the first tracheal rings, and exhibit a similar ovoid shape and overall volume as the lateral chambers observed in Hipposiderid, Rhinonycterid, and Rhinolophid bats (Figure 1). However, a notable distinction is the ventral opening of the chambers on the trachea of *Nycteris tragata*, in contrast to the dorsal opening observed in the two other bat families (Figure 1). Additionally, *Nycteris tragata* possesses only a single pair of chambers,

while variations in the number of chambers have been observed in Hipposiderid, Rhinonycterid, and Rhinolophid species, ranging from two to four chambers (Figure 1). Notably, no other bat clade exhibits chambers adjacent to their larynx.

Interspecific variation in tracheal chamber volumes

Among bats families, Hipposideridae and Rhinolophidae exhibit similar body masses despite the Hipposideridae having greater intraspecific variations, but the Rhinolophidae showcase a greater tracheal chamber volume, primarily due to larger lateral chambers relative to body mass (0.3345 mm^3/g versus 0.1429 mm^3/g, Figure S1). The dorsal pair of chamber volume, however, is similar for the two families. Nycteridae have similar average body mass and Frequency of Maximum Energy (FME) to Hipposideridae (Body mass: 23.8 g and 25.2 g, FME: 90 kHz and 114 kHz, Figure S1).

Coevolution of morphological and bioacoustical variables with tracheal chambers

Our linear model results indicate, generally, that as body mass or volume of tracheal chambers increases, FME tends to decrease (Tables 1 and S1). Notably, there is a linear increase in both body mass and chamber volume. When considering bats with chambers (D5), chamber volume has a greater impact on FME than does body mass, with the relationship between FME and body mass exhibiting a higher intercept (Tables 1 and S1). It is worth mentioning that most chamber volumes in D1 (the dataset including all species sampled; Table S1) are equal to zero due to the absence of chambers, yielding a non-significant result. FME and chamber volume covary more strongly (R^2 = 0.7749) than do FME and body mass (R^2 = 0.2781). Consequently, in our study, the presence or absence of tracheal chambers emerges as the primary factor influencing the linear relationship between FME and body mass (Table 1). Other variables such as guilds, laryngeal echolocating behaviours, or emission types do not significantly influence FME variations (Table 1).

158 Additionally, among bats with tracheal chambers (D5), the varying numbers of chambers do not
159 differentially impact FME variations (Table 1). We found a significant difference in FME emitted
160 between species without tracheal chambers ("0") and species with one or more tracheal chambers
161 (p = 0.0389, Figure 2, Table 1).
162
163 Correlated evolution models
164 *Rates of transitions*
165 The comparison of Akaike information criterion (AIC) and log-Likelihood (logLik) values
166 indicates that the Mk2 model (no loss of chamber and potential transition from two to four
167 chambers) provides the best explanation for the evolution and transitions of tracheal chambers
168 (Table S2). Therefore, the most probable scenario involves ordered gains of chambers without any
169 losses. On the other hand, the Mk4 model, which includes all potential transitions, receives less
170 support due to its greater complexity. The comparison between Mx1 and Mx2 models does not
171 reveal a significant difference, despite Mx2 incorporating different rates of transition. Notably, Mx2
172 exhibits transition values for chamber loss that are close to zero, indicating a lack of potential
173 chamber loss, similar to the Mk2 model for the diversification of tracheal chambers.
174
175 *Pagel's models*
176 The tests examining correlated evolution between tracheal chambers and the type of
177 emissions was conducted on D3 (dataset comprising all laryngeal echolocators and no other) and
178 the test for laryngeal echolocating behaviours was conducted on D4. The results for the type of
179 emission reveal a significant difference between the dependent and independent models (p =
180 0.0227). These results indicate potential coevolution of tracheal chamber acquisition and type of
181 emission. The transitions illustrated in the dependent model show that there are three main
182 combinations of states for bats, nasal emitter with or without tracheal chambers and oral emitter

without tracheal chambers (Figure 3, Table 2). The model with the laryngeal echolocation behaviours does not provide evidence to reject the independence of laryngeal echolocation behaviours from the acquisition of tracheal chambers, as indicated by non-significant p-value of the Pagel's test (Figure S2, Table 2). Notably, the transition representing the loss of chambers in this model exhibits a null value, consistent with the transition rates observed in the Mk2 and Mx2 models (Tables 2 and S2). Additionally, bats can transition from FM LDC behaviour to CF HDC behaviour; however, the traits display null values for the transition rates in the opposite direction (Figure S2).

Threshold models

The threshold models yield different results. Firstly, the model incorporating FME and tracheal chamber acquisition has a 95% confidence interval that includes only positive values (Table 2). This suggests significant correlation between these variables, indicating that individuals with tracheal chambers exhibit higher FME values. Secondly, the results of the threshold model for types of emission are similar to those of the Pagel's test, but the model results for laryngeal echolocation behaviours are different from those of the Pagel's test. Indeed, in both cases, the 95% confidence intervals exclusively contain negative values, which indicates that, for bats possessing tracheal chambers, they are most likely to be nasal emitters as well as emitting CF HDC calls, with a 95% confidence level. Therefore, both threshold models illustrate the dependence of the types of emission and laryngeal echolocating behaviours on the presence of tracheal chambers.

Ancestral state reconstruction (ASR)

ASR of tracheal chamber' acquisition

The marginal ancestral state reconstruction (ASRs) results for the complete data sampling (D1) reveal that tracheal chambers appeared twice in bat phylogeny. One of the appearances

208 occurred at the ancestor of the Nycteridae family, while the other occurred at the common ancestor
209 of the Rhinolophidae, Hipposideridae, and Rhinonycteridae families (Figure S3). The model
210 suggests that the ancestor of Rhinolophoidea did not possess tracheal chambers. No other
211 transitions of chambers are evident in the tree (Figure S3). The density map of the stochastic ASR
212 model yields similar results. It indicates two transitions throughout the entire tree, from the absence
213 of chambers to their presence, with no observed reverse transition (Figure 4). The transition period
214 for the acquisition of chambers in Nycteridae could have occurred as early as 50 million years ago
215 (mya), albeit with low probability, and had certainly occurred 12.5 mya before the diversification of
216 the family (Figure 4). In contrast, the transition is observed during the early Eocene for the crown
217 group of Rhinolophidae, Hipposideridae, and Rhinonycteridae. The marginal and stochastic models
218 for the diversification of chambers provides additional information regarding the timing and
219 location in the tree where the acquisition of a third and fourth chamber occurred (Figures 4 and
220 S3). Most species in Rhinolophidae, Hipposideridae, and Rhinonycteridae acquired a third and/or
221 fourth chamber (13 out of 18 species in our data), but no specific distribution pattern is evident.
222 The time of acquisition and the number of chambers vary among species within the same clade
223 (Figure 4). The tree illustrates that most nodes among the Rhinolophidae, Hipposideridae, and
224 Rhinonycteridae possess two tracheal chambers and that transitions from two chambers to more
225 occurred during the most recent speciation events.
226
227 *Comparison with the types of emission and laryngeal echolocating behaviours ASRs*
228 The marginal reconstruction of nasal and oral emitting strategies reveals that the common
229 ancestor of all laryngeal echolocating bats predominantly exhibited the oral emission trait. However,
230 a proportion of the state reconstruction suggests the presence of nasal emission for this common
231 ancestor (38.6%, Figure S3). The nasal emission trait is more widely distributed in Rhinolophoidea
232 and their ancestral nodes (except *Craseonycteris thonglongyai*), while the oral emission is widely

233 distributed in the Yangochiroptera and their ancestors except for Phyllostomidae and Nycteridae.
234 The nasal trait is greatly distributed compared to tracheal chamber acquisition and appears in
235 deeper roots of the tree. Contrarily, the CF HDC behaviour is less represented in the ancestral nodes,
236 primarily occurring in the most recent speciation events on the tree (Figures 4 and S3). The
237 common ancestor of Mormoopidae is reconstructed as FM LDC, with a transition to CF HDC
238 occurring only after speciation in *Pteronotus rubiginosus*. The common ancestor of all laryngeal
239 echolocating bats is reconstructed as an oral FM LDC emitter without chambers in these models,
240 but it should be noted that the models excluded the non-laryngeal echolocating Pteropodidae, so
241 this node's reconstruction is potentially biased. Similar to the tracheal chamber ASR models, we
242 observe different transitions (2 for laryngeal echolocation behaviours, 3 for types of emission)
243 occurring at different periods within different clades.
244
245 *Comparison with the FME and body mass ASRs*
246 The comparisons of evolutionary models on FME and body mass data indicate that their
247 evolution is best supported by a Brownian motion evolutionary model (Table S3, Figure S4). The
248 distribution of data across the bat phylogeny appears random, as no distinct groups are evident in
249 the phenograms (Figures S4 and S5). Compared to the rodent sample, bats exhibit a wide diversity
250 of size and FME, whereas rodent species have experienced an increase in body mass since their
251 common ancestor with bats.
252 The ASR trees reveal that the common ancestor of all bats possessed lower body mass, but
253 similar FME compared to the common ancestor of bats and rodents (Figure S4). The common
254 ancestor of Yinpterochiroptera shares similar body mass and FME with the common ancestor of all
255 bats (body mass: 17.455 $\pm$ 0.04 g, FME: 62.476 $\pm$ 0.002 kHz). Within the Yinpterochiroptera, the
256 ancestor of all Pteropodidae had lower FME and larger body mass than their ancestor shared with
257 Rhinolophoidea. Conversely, the common ancestor of all Rhinolophoidea appears to have higher

FME and smaller body mass than the Yinpterochiroptera common ancestor (Figure S4). The ancestor of all Yangochiroptera seems to have had similar FME to the Yinpterochiroptera ancestor but with a lower body mass, similar to the Rhinolophoidea. Variations in body mass primarily occur in the most recent nodes of the tree, while FME variations appear earlier. Most Hipposideridae species in the dataset exhibit extremely high FME, as do the two Natalidae species, *Kerivoula hardwickii*, and both Nycteridae species. On the other hand, Molossidae, Emballonuridae, and Pteropodidae evolved with a lower frequency of sound production. Rhinolophidae species show greater variability, with some displaying high FME and others low FME (Figure S4). Therefore, interpretation of the ASRs for body mass and FME is limited.

The small variations observed in FME can be partially attributed to the presence and volume of chambers in Rhinolophoidea and Nycteridae species, as their body size is not consistently small compared to other bat species. Two transitions from the absence to the presence of tracheal chambers have been identified in the bat phylogeny, but a similar pattern of variation is not observed for FME, as more species are transitioning to lower FME than their ancestors.

Discussion

We hypothesized that tracheal chambers, within the larynx, may have facilitated laryngeal echolocation capabilities in bats, a trait that is undoubtedly responsible for their evolutionary success and for their adaptation to and distribution in different environments worldwide. Using the first multi-modal approach to uncover the evolutionary history of tracheal chambers, we found correlations between their acquisition, nasal emission, and high-frequency sound production. Among Rhinolophoidea, we found the acquisitions of chambers to be concomitant with CF HDC echolocation behaviour, and that the increase in number of chambers does not affect the FME. We propose that tracheal chambers represent a key innovation in chiropteran evolutionary history,

enabling specific laryngeal echolocation specialisation, and potentially supporting niche diversification.

Tracheal chamber and Frequency

FME and body mass have occasionally been shown to coevolve in mammals (Dunn et al., 2015; Bowling et al., 2017), and our findings demonstrate that this relationship holds true for bats, particularly for species heavily reliant on sound emission. The FME of bat species does not appear to be significantly impacted by factors such as guild, laryngeal echolocating behaviours, or types of emissions. We found that the presence of tracheal chambers in nasal emitting bats correlates with higher FME, in addition to the effect of body mass (Castro et al., 2024). This relationship follows a similar linear pattern to that for bats without chambers, but with a higher intercept, suggesting that the presence of tracheal chambers enables bats to produce higher frequencies. The number of tracheal chambers does not significantly affect FME (Figure 2), and dorsal tracheal chambers, when developed, represent a small portion of the tracheal chambers (less than 20% of the total volume for most species). Therefore, dorsal chambers might not directly be involved in FME regulation. It has been previously suggested that dorsal chambers play a role in CF HDC specialization by amplifying the emitted frequency without modifying the pitch or FME (Au and Suthers, 2014; Ma et al., 2016). The presence of dorsal chambers in CF HDC Rhinolophoidea and their absence in FM LDC Nycteridae species support this proposition.

Evolutionary patterns of tracheal chambers

The MK2 model revealed that acquiring the first pair of tracheal chambers is an unlikely event in bat evolution, with a low transition rate. However, a higher transition rate indicates that bats possessing lateral tracheal chambers are more likely to gain dorsal tracheal chambers. We also confirmed in some species that the previously thought unique third tracheal dorsal chamber is an

307 unseparated pair of dorsal chambers, even in fully mature individuals (Brualla et al., 2024; Nojiri et
308 al., 2024). This biological pattern aligns with the bilaterian symmetric anatomical scheme of tracheal
309 chamber development. Nojiri et al. (2024) described the symmetrical development of chambers
310 during bat ontogeny, explaining that "condensed chondrocytes in both the lateral and dorsal
311 tracheal chambers were separated to form the left and right tracheal chambers". Therefore, the
312 third chamber observed in several bat species represent a non-separation of the chondrocytes
313 during development, resulting in a fused pair of dorsal chambers. Additionally, the loss of tracheal
314 chambers is unlikely to occur, as indicated by the zero transition rate in the Mk and Pagel's models
315 (Tables 2 and S2).

316 We described tracheal chambers in the Rhinolophidae and Hipposideridae, and
317 Rhinonycteridae species. They are absent from the three other families of Rhinolophoidea
318 (Megadermatidae, Craseonycteridae, and Rhinopomatidae). From a phylogenetic perspective, this
319 illustrates an acquisition of chambers after the separation of the two clades among Rhinolophoidea
320 (Figures 4 and S3). All Rhinolophoidea are capable of producing CF calls (Surlykke et al., 1993;
321 Leippert et al., 2000; Fenton et al., 2012), but solely the Rhinolophidae, Hipposideridae and
322 Rhinonycteridae are HDC emitters. Therefore, this might indicate that tracheal chambers support
323 the specialisation of bats as HDC emitters in Rhinolophoidea.

324 In Nycteridae, the lateral tracheal chambers originate from the ventral part of the larynx
325 (Figure 1). In contrast, tracheal chambers originate on the dorsal part of the larynx in the
326 Rhinolophoidea clade ("rostral" position in Nojiri et al., 2024). It was once hypothesised that
327 tracheal chambers were formed by the modification of the tracheal rings (Denny, 1976), but recent,
328 detailed developmental observations on *Rhinolophus pusillus* demonstrated that the condensed
329 chondrocyte mass comprising the lateral chambers originates from the caudal portion of the
330 cricoid cartilage, while the tracheal rings had not yet chondrified (Nojiri et al., 2024). Thus, it is most
331 likely that the lateral and dorsal tracheal chambers are a derivative of some parts of the cricoid

cartilage. Ancestral state reconstructions suggest that tracheal chambers in Nycteridae and in CF HDC bats of Rhinolophoidea have evolved convergently. However, it is not possible to conclude whether the tracheal chambers in the two separate lineages are anatomically homologous structures. To resolve this question, future investigation on the morphogenesis of the tracheal chambers in Nycteridae is necessary.

Tracheal chamber are a key innovation of nasal emission and high duty cycle specialisation

Here, we propose evolutionary scenarios to elucidate the presence of tracheal chambers and their interaction with other factors related to laryngeal echolocation. Our Pagel's, threshold, marginal, and stochastic models confirm that nasal emission likely emerged earlier in bat evolutionary history than the development of tracheal chambers, thus explaining the broader distribution of nasal emitters (Figure 6). Nevertheless, we found dependent coevolution between the two variables. Consequently, a hierarchical relationship may exist, where bats with chambers are consistently nasal emitters, but nasal emitters do not always possess tracheal chambers. The development of chambers appears to be more closely associated with the need to produce higher FME as nasal emitters, rather than solely for nasal laryngeal echolocation. This observation aligns with Phyllostomidae, which lack tracheal chambers and are known as "whispering bats," as they produce calls with low frequency and amplitude (Ma et al., 2016). Notably, when chamber volumes are high in some Rhinolophidae, the emitted frequency decreases (Figure S1), possibly because larger volumes involve the production of lower frequencies in comparison to other species with smaller tracheal chambers. Another potential functional adaptation could be to regulate heat and water retention during respiration in the nasal cavities (Dzal and Gillam, 2023), which may be confirmed by future study that investigates the entire vocal tract. This exploration could help to fully understand the potential role of the tracheal chambers.

356 The independence of tracheal chambers from CF HDC behaviours found through the
357 Pagel's test results is reflected by bats that produce CF HDC calls (*P. rubiginosus*) lacking chambers.
358 Nevertheless, the negative values of the correlated evolution in the threshold test for echolocation
359 behaviour, as well as the presence of dorsal chambers only in CF HDC Rhinolophoidea, indicate a
360 potential relationship between tracheal chambers and CF HDC in Rhinolophoidea. We propose that
361 the specialization for CF HDC echolocation may not require identical functional adaptations for
362 nasal and oral emitters. In the evolution of nasal Rhinolophoidea, we demonstrated that the
363 development of tracheal chambers only appeared in HDC emitters. Rhinolophidae have the highest
364 HDC of all bats (≈ 50% of call time is sound emitted; Fenton et al., 2012) and we show that these
365 bats possess the most voluminous lateral chambers relative to body mass and dorsal chamber
366 volume (Figure S1). Lateral chambers filter the fundamental frequencies, improving the FME signal
367 on the second harmonic (Ma et al., 2016). Therefore, we propose that larger lateral chamber
368 volumes are found in highly specialised HDC CF bats such as Rhinolophidae because these
369 chambers could enable a better filtering system during sound production in cluttered
370 environments. We also propose that an increase in lateral chamber volume might enable
371 Rhinolophidae to produce longer CF calls in flight by storing a reserve quantity of air that could
372 supplement the air from the lungs. This would enable higher HDC ratio, at a cost of the slightly
373 lower FME (Figures S1 and S4). On the other hand, dorsal chambers contribute to increase sound
374 amplitude by reflecting emitted sound in the trachea, thus improving the CF HDC specialisation
375 (Au and Suthers, 2014; Ma et al., 2016). Dorsal tracheal chambers are, nonetheless, variably present
376 in CF HDC Rhinolophoidea and their exact role remains therefore debatable. The coevolutionary
377 trend between tracheal chambers and CF HDC specialisation potentially arose because the
378 common ancestor of all Rhinolophoidea was already a nasal emitter. Later, tracheal chambers
379 appeared in the common ancestor of Rhinolophidae, Hipposideridae, and Rhinonycteridae and not
380 in the other families. We suggest that nasal emission may have induced the functional adaptation

through development of tracheal chambers for CF HDC production, due to attenuation of call intensity going through the nares. Their contribution to sound intensity and duration would explain why all CF HDC nasal emitters possess tracheal chambers (Roberts, 1972; Denny, 1976). *Pteronotus rubiginosus*, a distantly related species outside the Rhinolophoidea, is an oral emitter capable of CF HDC echolocation without possessing tracheal chambers. Consequently, we propose that oral emission imposes fewer restrictions on the functional adaptations for sound production. Therefore, *P. rubiginosus* was able to recently specialize as a CF HDC echolocator without the necessity of tracheal chambers, as supported by the ASR models (Figures 4 and S3).

From an evolutionary perspective, we suggest that nasal emitters of the Old World, potentially forced by environmental pressures, adapted through speciation to different ecological niches. In both Rhinolophoidea and Nycteridae, lateral tracheal chambers might have been the morphological adaptation that allowed this ecological transition with the potential to produce higher FME. In the Rhinolophoidea, lateral tracheal chambers also helped bats to reach new ecological opportunities through a second functional adaptation with the specialisation in CF HDC. We can observe this transition with all the CF HDC Rhinolophoidea being part of the NSFD guild (active flutter detecting), compared to the remaining Rhinolophoidea being mostly passive gleaners (NSPG guild; Denzinger and Schnitzler, 2013). CF HDC echolocation allows these bats to be active hunters and compensate for the Doppler effect in cluttered environment. In recent times, these same bat families speciated and evolved to develop dorsal tracheal chambers (Figures 1 and 4). These chambers might have been used to improve the CF HDC behaviour through amplification of the sound emitted. Regarding the Nycteridae, they remained passive gleaners, which correlates with the presence of only lateral tracheal chambers. Nycteridae might benefit from the presence of tracheal chambers only to produce higher FME as nasal emitter. Therefore, we suggest that tracheal chambers represent a diversifying trait in Nycteridae evolution, and a key innovation for

the Rhinolophidae, Hipposideridae and Rhinonycteridae. Further studies with broader sampling may seek to confirm this assertion.

Resource availability:

Lead contact:

Further information and request to access resources used in this study should be addressed directly to the main corresponding author, Dr Daisuke Koyabu (dsk8evoluxion@gmail.com).

Materials availability:

This study did not generate new unique reagents.

Acknowledgements:

This study was supported by City University of Hong Kong Start-up Grant (9610466), JSPS (21H02546, 21K19291, and 22KK0101), JST (JPMJFR2148) to D.K., and a grant from the Australian Research Council to L.A.B.W. (FT200100822).

Author contributions:

Conceptualisation, NLMB, LAB, DK; methodology, NLMB, LAB; software, NLMB; investigation, NLMB; resources, NLMB, LAB, KH, VTT, TN, TW, and DK; visualisation, NLMB; supervision, LAB, MD, DK; writing – original draft, NLMB; writing – review and editing, NLMB, LAB, KH, MD, VTT, TN, TW, and DK.

Declaration of interests:

The authors declare no competing interests.

Figures

Figure 1: Cranial and right lateral views of 3D reconstruction of the cricoid cartilage, trachea, and tracheal chambers in *Rattus norvegicus domestica*, *Eonycteris spelaea, Rhinolophus cornutus, Hipposideros larvatus,* and *Nycteris tragata.*

Figure 2: Linear regressions of frequency of maximum energy (FME) with body mass, depending on the number of tracheal chambers present (logged axes). Also see Figure S1 and Table S1.

Figure 3: Different correlated evolution models of the tracheal chambers and the type of emissions. a), dependent model; b), independent model. Arrows indicate the direction and rates of transition between states. Also see Table 2A and Figure S2.

Figure 4: Ancestral state reconstructions (ASR) of different biological traits in bats. See also Figure S3, S4 and S5. See also Table S2. A to C models are density maps of the stochastic models, D displays the percentages at each node of the stochastic model. The green star illustrates the common ancestor of all Rhinolophidae, Hipposideridae and Rhinonycteridae. A, ASR of the tracheal chambers acquisition with Dataset 1; B, ASR of the type of emission with Dataset 3; C, ASR of the laryngeal echolocating strategies with Dataset 3; D, ASR of the diversification of tracheal chambers with Dataset 1. ABS, absence of chamber; PRES, presence of chambers; CF, constant frequency calls; FM, frequency-modulated calls; Pa, Paleocene; Oli, Oligocene; P, Pliocene; Q, Quaternary.

Tables

Table 1: Phylogenetic generalized least squares of frequency of maximum energy (FME) and body mass (BM) testing the potential influence of different variables. TCV, tracheal chamber volume; TC, tracheal chambers; LE, laryngeal echolocation.

Model	PGLS	Anova/Ancova
FME/BM + TCV (TC)	BM = 0.0594 TCV = **0.0002**	BM = **1e-04** TCV = **2e-04**
FME/BM + TCV (all)	BM = **0.0002** TCV = 0.7868	BM = **0.0001** TCV = 0.7868

Model	PGLS	Anova/Ancova
Tracheal Chambers (all)	BM = **0** TC = **0.004**	BM = **<0.0001** TC = **0.004**
TC Number (TC)	BM = 0.0538 Others > 0.05	BM = **0.0178** Others = 0.8547
TC Number (all)	BM = **0** Others > 0.05	BM = **<0.0001** NTC = **0.0389**
LE strategies	BM = **0.0018** Others > 0.05	BM = **0.0001** ST = 0.3429
Nasal/Oral emission	BM = **0.0002** Others > 0.05	BM = **<0.0001** NO = 0.0824
Guilds groups	BM = **0.0004** Others > 0.05	BM = **0.0001** GD = 0.1810

Table 2: Correlated evolution models. Also see Figure 3 and Figure S2. A. Results from the Pagel's models. B. Results from the Threshold models. AIC, Akaike information criterion; CI, confidence interval; FME, frequency of maximum energy; NO, type of emission (nasal or oral); ST, strategies of laryngeal echolocation; TC, tracheal chambers.

463 A.

Test	Model	Log-likelihood	AIC	P-value
TC – NO All except "none"	Independent	-23.56711	55.1342	**0.0227**
	Dependent	-17.8766	51.7533	
TC – ST	Independent	-17.1538	42.3077	0.0829
	Dependent	-13.0294	42.0588	

464 B.

Trait 1	Trait 2	Lower limit 95% CI	Higher limit 95% CI
FME	TC	0.0044	0.7950
TC	Emission Type	-0.9203	-0.0830
TC	Echolocation Behaviour	-0.8966	-0.1095

465

466

467

468

STAR Methods

Key resources table

Experimental model and study participant details

Dataset

Our total sampling includes 54 species, representing 51 species of bats and 3 species of rodents as an outgroup. Among the bat sample, we collected six Pteropodidae, 12 Hipposideridae, one Rhinonycteridae, five Rhinolophidae, two Megadermatidae, one Rhinopomatidae, one Craseonycteridae, two Nycteridae, three Emballonuridae, four Phyllostomidae, three Mormoopidae, two Noctilionidae, two Molossidae, one Miniopteridae, four Vespertilionidae and two Natalidae. This constituted the main sample D1 (Table S4). Specimen were sourced from different institutions:

Phylogenetic relationships among the species sampled in this study were obtained from the Timetree database (Kumar et al., 2022), using the adjusted time of speciation between each taxon. The phylogenetic tree has been built using Mesquite software (Maddison and Maddison, 2007). To discuss evolutionary history of the different laryngeal echolocation strategies among bats, our sampling approach encapsulates all combinations of laryngeal echolocating behaviours among Yinpterochiroptera and Yangochiroptera suborders (constant frequency or frequency modulated emitters, and low-duty or high-duty cycle sound producers). We also selected species depending on their sound emission types (nasal or oral), and by their distribution in guilds defined previously by Denzinger and Schnitzler (2013). By including bats with and without tracheal chambers, we sought to explore potential correlations between chamber presence, morphology, and variations in sound production (sound frequency, nasal or oral emission, laryngeal echolocating behaviours).

Method Details

Data acquisition and measurements

Iodine contrast-enhanced X-ray microtomography ("diceCT") (Metscher, 2009; Gignac et al., 2016) was used to make three-dimensional reconstrcutions of the laryngeal cartilages of four species of the Rhinolophid family, nine species of Hipposiderids and one species of Nycterids from the total sampling to represent laryngeal echolocating species with tracheal chambers in a subsample (D5; Table S4). We added 3D surfaces of one specimen of the Pteropodid family, *Eonycteris spelaea* and one Muridae (*Rattus norvegicus domestica*) to anatomically compare the larynx and trachea of bats and non-bat small mammals (Table S4). Visualization and segmentation were performed using AMIRA 5.3.3 software (ThermoFisher). Isotropic pixel spacing between 10 and 30 µm was used, providing sufficient resolution for segmentation (Brualla et al., 2024). We described the tracheal chambers of *Nycteris* in detail for the first time, whose chambers have been only briefly mentioned in Denny (1976) and illustrated in Griffiths' drawings (1994).

The tracheal chamber volume was measured using Morphodig software (Lebrun, 2018). Three volume variables were defined: total chamber volume, lateral chamber volume, and dorsal chamber volume. To compare the impact of tracheal volume on sound frequencies while considering the size of individuals, average body masses of all bats were obtained from external sources, such as the Global Biodiversity Information Facility website (GBIF, www.gbif.org) (Table S6). The frequency of maximum energy (FME) for each species was collected from the authors' recordings, as well as from external sources such as Furey et al. (2009) and Hughes et al. (2011). Additional FME data were obtained from audio recordings available in public online audio libraries Chirovox and Morcegoteca (Appel et al., 2016; Görföl et al., 2022) (Table S6). Unfortunately, some FME were not found for several species, reducing the species number from the original dataset (D1 with 53 species) to 48 species for several tests (D2; Tables S4 and S5). Acquisition of information on emission types (nasal or oral emitting bats) also reduced the sampling size from 48 to 44 species,

by removing outgroups and Pteropodidae that do not laryngeally echolocate (D3; Table S4). Several tests of this study required binary traits to function (e.g., Pagel's models for correlated evolution) and constrained the dataset size from 44 species to 35 species when selecting only bats with the two main laryngeal echolocating behaviours (CF HDC or FM LDC) (D4; Tables S4 and S5). These samplings allowed for comparisons and evolutionary discussions to be made between vocal production parameters, body size and the variations in tracheal chamber numbers and volumes.

Quantification and Statistical analyses

Data analyses

All categorical and continuous data about tracheal chambers and laryngeal echolocation were imported into Rstudio software (R version 4.3.1; Posit Team, 2024) for further analyses (Table S6). We first described the differences in FME compared to the body mass and the different chamber volumes using D5 to visualise the different relations between size and sound frequency in bats with chambers. We used boxplots and biplots to summarize body mass, frequency and chamber volume data by family. Additional comparisons of the FME and body mass on D2 dataset were realized.

PIC and PGLS

Looking for correlation and coevolution between FME, body mass and tracheal chambers was essential. Considering the phylogeny, we ran phylogenetic independent contrasts (PIC) analyses between the three variables, for all species with FME (D2), then only for species of the D5 to observe if a potential correlation was only visible in bats possessing tracheal chambers. Other biological factors such as the guilds, the laryngeal echolocation behaviours (such as CF HDC) and the type of emission (nasal or oral emitters) might influence FME variation and the presence or absence of chambers and their volume. Phylogenetic generalized least squares (PGLS) coupled with

Anova/Ancova have been used to test the different biological variables against the negative and linear relation between FME and body mass.

Evolutionary rates for tracheal chambers

We investigated the evolutionary rate of tracheal chamber appearance among bats, using Mk (Markov k-state) models with discrete characters on D1 sample. Mk models consider the tracheal chambers as having a finite and discrete number of possible transitions between stages. We used the package "geiger" (Pennell et al., 2014) and a phylogenetic tree including all species of D1 (package "ape"; Paradis and Schliep, 2019). We resolved all potential polytomies using the function multi2di() from the "ape" package. We coded the variable by the number of chambers present ("0","2","3", and "4") excluding the stage "1" because no bat species has only one tracheal chamber. We proposed four different evolutionary scenarios for the transitions from one state to another. The first model (Mk1) accepted only gain of chambers (impossible to have a loss) and the transitions were ordered from zero to four. The second model (Mk2) was identical to the first model, but it was possible to transition directly from two chambers to four chambers. The third model (Mk3) was ordered like the first model, but we included the possibility to lose chambers at each stage, so that each transition could be a gain or a loss of chambers. Lastly, the fourth model (Mk4) accepted all possible transitions from any stage to another, as a gain or a loss. We tested the differences of likelihood of these models to assess whether one model could outperform the others and better (but not fully) explain the evolutionary history of the tracheal chamber diversification in bats. We added two models for the acquisition or loss of the tracheal chambers, one with equal rate of transition (Mx1) and one with different rate between acquisition and loss (Mx2).

Correlated evolution of variables

We ran Pagel's models to test the evolutionary independence of the development of tracheal chambers to the adaptation to nasal or oral emissions and to the two main laryngeal echolocation behaviours (CF HDC and FM LDC), using the D3 and D4 respectively (Tables S4 and S5). As these models run binary variables, we had to select the two main laryngeal echolocating behaviours. In addition, we ran Threshold models on the different datasets to assess the impact of implementing a continuous approach for discrete traits (Table S5). Testing the independence of the traits, with the addition of the PGLS results, allow us to test whether the reconstruction of tracheal chamber evolutionary history can be a good proxy to reconstruct the ancestral states and evolutionary history of different laryngeal echolocating parameters.

Ancestral state reconstruction (ASR)

Lastly, we investigated the discrete reconstruction of the ancestral states for the tracheal chambers. We use marginal and stochastic ancestral state reconstruction (ASR) models on different datasets to understand the acquisition and diversification of tracheal chambers (D1), the diversification of the type of emissions (D3) and of the laryngeal echolocating behaviours (D4). Marginal models allow to obtain ASRs by calculating the maximum likelihood of each node in the tree during reconstruction, instead of a general likelihood for the reconstructed tree like in Mk models. Stochastic models allow consideration of probabilities of occurrence with a Bayesian approach, and potential transitions along branches and not only at specific nodes. We used the functions corHMM() of the package "corHMM" for the marginal models and make.simmap() function from "phytools" package for the stochastic models (Beaulieu et al., 2022; Revell, 2024). For the stochastic ASR, we ran 10 000 iterations to produce sufficient reconstructions, encompass the different potential scenarios, and obtain supported probabilities. We summarised the results in one density map by averaging the results of 1000 of the reconstructed trees, each picked every 10

589 iterations. To further characterise the relationship between tracheal chambers and FME produced
590 by bats, we ran an ASR continuous model for FME and body mass on species from D2 using the
591 functions fitContinuous ("geiger" package), fastAnc, and contMap ("phytools" package).
592 Beforehand, we tested which model would best fit our data (Brownian Motion, Early Burst or
593 Ornstein-Uhlenbeck). As the distribution of body masses in the dataset was not normally
594 distributed, a $\log_e$ transformation was applied before running the tests for evolutionary model
595 comparisons. We observed the topography of ancestral states trees for FME and tracheal chambers
596 to assess whether these features potentially coevolved. Additionally, we could discuss whether the
597 tracheal chambers should be considered as key innovations or diversifying traits. If we successfully
598 determine that tracheal chambers coevolve with FME or other laryngeal echolocation parameters,
599 we might use the ASR of tracheal chambers to deduce the evolutionary history of laryngeal
600 echolocation in bats. Therefore, we could conclude that tracheal chambers allowed bats to reach
601 new ecological niches through laryngeal echolocation specialisation and to potentially speciate in
602 numerous new species.

603 References

604 Appel G, Pathek DB, Di Ponzio R, Colombo GT, López-Baucells A, Bobrowiec PED. 2016
605 MORCEGOTECA: biblioteca virtual de ultrassons de morcegos. CENBAM, PDBFF, Manaus, Amazonas,
606 Brasil.
607 Au WW, Suthers RA. 2014 Production of biosonar signals: Structure and form. Biosonar. Vol.
608 51. Springer New York. pp. 61-105. https://doi.org/10.1007/978-1-4614-9146-03
609 Beaulieu J, O'Meara B, Oliver J, Boyko J. 2022 corHMM: Hidden Markov Models of Character
610 Evolution. R package version 2.8, https://CRAN.R-project.org/package=corHMM
611 Bowling DL, Garcia M, Dunn JC, Ruprecht R, Stewart A, Frommolt K-H, Fitch WT. 2017 Body
612 size and vocalization in primates and carnivores. Sci. Rep. Vol. 7 pp. 1–11.
613 https://doi.org/10.1038/srep41070
614 Brualla NL, Wilson LA, Tu VT, Nojiri T, Carter RT, Ngamprasertwong T, Wannaprasert T, Doube
615 M, Fukui D, Koyabu D. 2024 Comparative anatomy of the vocal apparatus in bats and implications
616 for the diversity of laryngeal echolocation. Zool J Linn Soc. zlad180.
617 https://doi.org/10.1093/zoolinnean/zlad180
618 Brualla NLM, Wilson LA, Doube M, Carter RT, McElligott AG, Koyabu D. 2023 The vocal
619 apparatus: An understudied tool to reconstruct the evolutionary history of echolocation in bats?. J
620 Mamm Evol. Vol. 30(1). pp. 79-94. https://doi.org/10.1007/s10914-022-09647-z
621 Carter RT. 2020 Reinforcement of the larynx and trachea in echolocating and non-
622 echolocating bats. J Anat 237(3):495–503. https://doi.org/10.1111/joa.13204
623 Castro MG, Amado TF, Olalla-Tárraga MÁ. 2024 Correlated evolution between body size and
624 echolocation in bats (order Chiroptera). BMC Ecol Evol. Vol. 24(1). https://doi.org/10.1186/s12862-
625 024-02231-4
626 DeMIGUEL D, Azanza B, Morales J. 2014 Key innovations in ruminant evolution: a
627 paleontological perspective. Integr Zool. Vol. 9(4). pp. 412-33. https://doi.org/10.1111/1749-
628 4877.12080
629 Denny SP. 1976 The bat larynx. In: Hinchcliffe R, Harrison DF (eds) Scientific Foundations of
630 Otolaryngology. Heinemann Medical Books, London, UK, pp 346–370
631 Denzinger A, Schnitzler H-U. 2013 Bat guilds, a concept to classify the highly diverse
632 foraging and echolocation behaviors of microchiropteran bats. Front Physiol 4:164.
633 https://doi.org/10. 3389/fphys.2013.00164
634 Dunn JC, Halenar LB, Davies TG, Cristobal-Azkarate J, Reby D, Sykes D, Dengg S, Fitch WT,
635 Knapp LA. 2015 Evolutionary trade-off between vocal tract and testes dimensions in howler
636 monkeys. Curr. Biol. Vol. 25. pp. 2839–2844. https://doi.org/10.1016/j.cub.2015.09.029
637 Dzal YA & Gillam EH. 2023 The nose knows: a review of the diversity, form, and function of
638 the external and internal features of the bat nose. Canadian Journal of Zoology. Vol. 102. pp. 103–
639 112.

Elias H. 1907 Zur anatomie des Kehlkopfes der Mikrochiropteren. Morphol Jahrb 37:70–119

Fenton MB, Faure PA, Ratcliffe JM. 2012 Evolution of high duty cycle echolocation in bats. J Exp Biol 215(17):2935–2944. https://doi.org/10.1242/jeb.073171

Fenton MB. 2013 Evolution of echolocation. Bat evolution, ecology, and conservation. Vol. 8. Springer New York. pp. 47-70. https://doi.org/10.1007/978-1-4614-7397-8_3

Furey NM, Mackie IJ, Racey PA. 2009 The role of ultrasonic bat detectors in improving inventory and monitoring surveys in Vietnamese karst bat assemblages. Curr Zool. Vol. 55(5). pp. 327-341. https://doi.org/10.1093/czoolo/55.5.327

Gignac PM, Kley NJ, Clarke JA, Colbert MW, Morhardt AC, Cerio D, Cost IN, Cox PG, Daza JD, Early CM, Echols MS, Henkelman RM, Herdina AN, Holliday CM, Li Z, Mahlow K, Merchant S, Müller J, Orsbon CP, Paluh DJ, Thies ML, Tsai HP, Witmer LM. 2016 Diffusible iodine-based contrast-enhanced computed tomography (diceCT): an emerging tool for rapid, high-resolution, 3-D imaging of metazoan soft tissues. J Anat 228(6):889–909. https://doi.org/10.1111/joa.12449

Gillet A, Frédérich B, Parmentier E. 2019 Divergent evolutionary morphology of the axial skeleton as a potential key innovation in modern cetaceans. Proc Biol Sci. 286(1916):20191771. https://doi.org/10.1098/rspb.2019.1771

Görföl T, Huang JC, Csorba G, Győrössy D, Estók P, Kingston T, Szabadi KL, McArthur E, Senawi J, Furey NM, Tu VT. 2022 ChiroVox: a public library of bat calls. PeerJ. Vol. 10:e12445. https://doi.org/10.7717/peerj.12445

Griffiths TA. 1994 Phylogenetic systematics of slit-faced bats (Chiroptera, Nycteridae): based on hyoid and other morphology. Am Mus Novit 3090:1–17

Harrison DFN. 1995 The Anatomy and Physiology of the Mammalian Larynx, 1st ed. Cambridge University Press, Cambridge, UK

Hartley DJ, Suthers RA. 1988 The acoustics of the vocal tract in the horseshoe bat, Rhinolophus hildebrandti. J Acoust Soc Am. Vol. 84(4). pp. 1201-1213. https://doi.org/10.1121/1.396621

Hughes AC, Satasook C, Bates PJ, Soisook P, Sritongchuay T, Jones G, Bumrungsri S. 2011 Using echolocation calls to identify Thai bat species: Vespertilionidae, Emballonuridae, Nycteridae and Megadermatidae. Acta Chiropterologica. Vol. 13(2). pp. 447-455. https://doi.org/10.3161/150811011X624938

Kumar S, Suleski M, Craig JE, Kasprowicz AE, Sanderford M, Li M, Stecher G, Hedges SB. 2022 TimeTree 5: An Expanded Resource for Species Divergence Times. Mol Biol Evol. Vol. 39(8). https://doi.org/10.1093/molbev/msac174

Langevin P, Barclay RM. 1990 *Hypsignathus monstrosus*. Mamm Species 357:1–4

Lebrun R. 2018 MorphoDig, an open-source 3D freeware dedicated to biology. IPC5 The 5th International Palaeontological Congress.

Leippert D, Goymann W, Hofer H, Marimuthu G, Balasingh J. 2000 Roost-mate communication in adult Indian false vampire bats (Megaderma lyra): an indication of individuality

678 in temporal and spectral pattern. Anim Cogn. Vol. 3. pp. 99-106.
679 https://doi.org/10.1007/s100710000067
680 Ma X, Li T, Lu H. 2016 The acoustical role of vocal tract in the horseshoe bat, Rhinolophus
681 pusillus. J Acoust Soc Am. Vol. 139(3). pp. 1264-1271. https://doi.org/10.1121/1.4944573
682 Maddison W, Maddison D. 2007 "Mesquite 2." *A modular system for evolutionary analysis* 3
683 Metscher BD (2009) MicroCT for comparative morphology: simple staining methods allow
684 high-contrast 3D imaging of diverse non-mineralized animal tissues. BMC Physiol 9(1):1–14.
685 https://doi.org/10.1186/1472-6793-9-11
686 Metzner W, Schuller G. 2010 Vocal control in echolocating bats. In: Brudzynski SM (ed)
687 Handbook of Behavioral Neuroscience. Elsevier, London, UK, pp 403–415
688 Miller AH, Stroud JT, Losos JB. 2023 The ecology and evolution of key innovations. Trends
689 Ecol Evol. Vol. 38(2). pp.122-31. https://doi.org/10.1016/j.tree.2022.09.005
690 Nojiri T, Takechi M, Furutera T, Brualla NL, Iseki S, Fukui D, Tu VT, Meguro F, Koyabu D. 2024
691 Development of the hyolaryngeal architecture in horseshoe bats: insights into the evolution of the
692 pulse generation for laryngeal echolocation. Evodevo. Vol. 15(1). https://doi.org/10.1186/s13227-
693 024-00221-7
694 Paradis E, Schliep K. 2019 ape 5.0: an environment for modern phylogenetics and
695 evolutionary analyses in R. Bioinformatics. Vol. 35. pp. 526-528.
696 https://doi.org/10.1093/bioinformatics/bty633
697 Pennell MW, Eastman JM, Slater GJ, Brown JW, Uyeda JC, FitzJohn RG, Alfaro ME, Harmon
698 LJ. 2014 geiger v2.0: an expanded suite of methods for fitting macroevolutionary models to
699 phylogenetic trees. Bioinformatics, 30, 2216-2218.
700 Posit team. 2024 RStudio: Integrated Development Environment for R. Posit Software, PBC,
701 Boston, MA. http://www.posit.co/
702 Revell LJ. 2024 phytools 2.0: an updated R ecosystem for phylogenetic comparative
703 methods (and other things). PeerJ. Vol. 12:e16505.
704 Roberts LH. 1972 Variable resonance in constant frequency bats. J Zool 166(3):337–348.
705 https://doi.org/10.1111/j.1469-7998.1972.tb03103.x
706 Robin HA. 1881 Recherches anatomiques sur les mammifères de l'ordre des chiroptères.
707 Dissertation, Faculté des Sciences de Paris Saigusa H (2011) Comparative anatomy of the larynx
708 and related structures. Jpn Med Assoc J 54(4):241–247
709 Schneider R. 1964 Der Larynx der Säugetiere. Handbuch Der Zoologie. Vol. 7. De Gruyter &
710 Co. Berlin. pp. 1-128.
711 Simmons NB, Cirranello AL. 2020 Bats of the world: a taxonomic and geographic database.
712 American Museum of Natural History.
713 Surlykke A, Miller LA, Møhl B, Andersen BB, Christensen-Dalsgaard J, Buhl Jørgensen M.
714 1993 Echolocation in two very small bats from Thailand Craseonycteris thonglongyai and Myotis
715 siligorensis. Behav Ecol Sociobiol. Vol. 33. pp. 1-12. https://doi.org/10.1007/BF00164341

716 Veselka N, McErlain DD, Holdsworth DW, Eger JL, Chhem RK, Mason MJ, Brain KL, Faure PA,
717 Fenton MB (2010) A bony connection signals laryngeal echolocation in bats. Nature 463(7283):939–
718 942. https://doi.org/10.1038/nature08737

Figure 1:

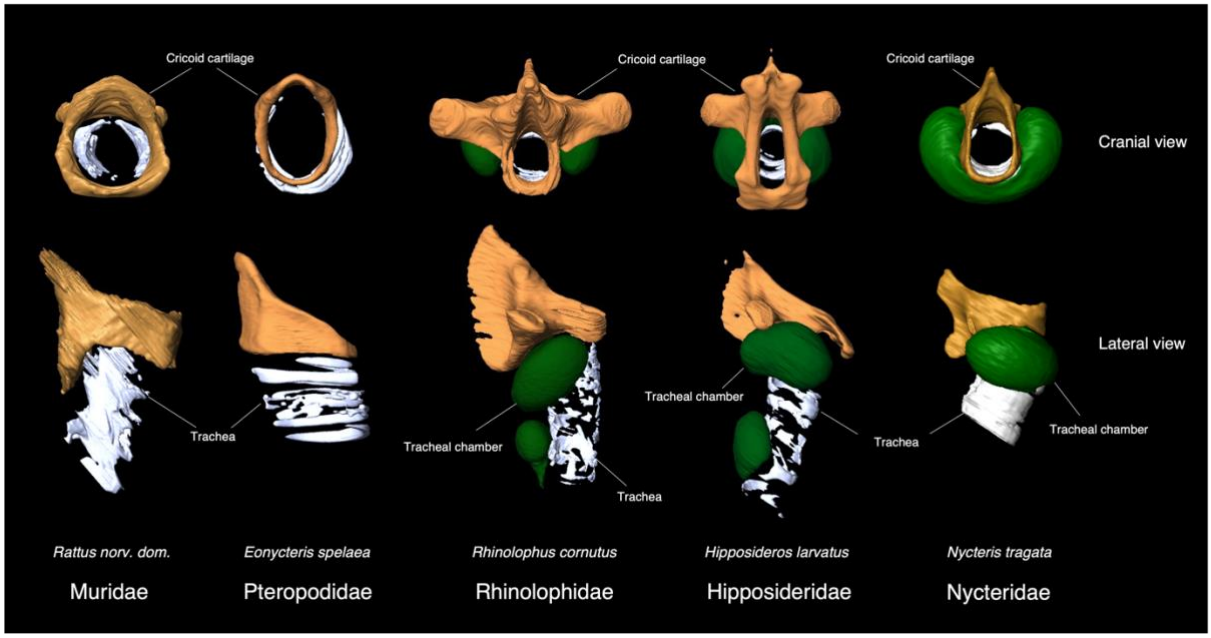

Figure 2:

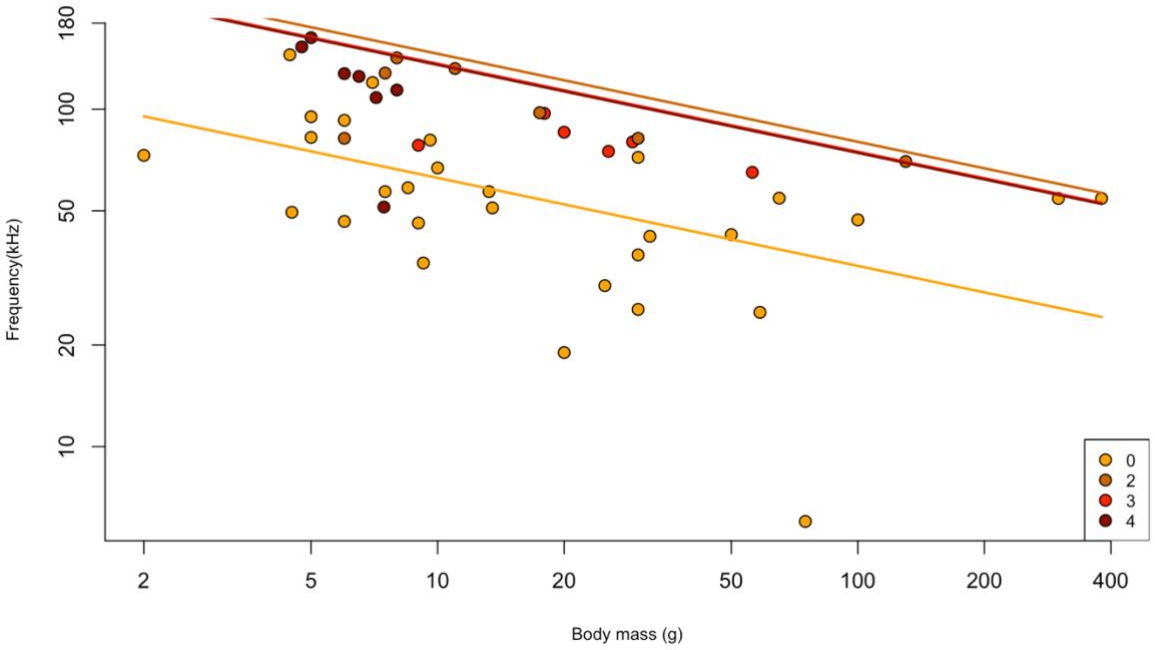

Figure 3:

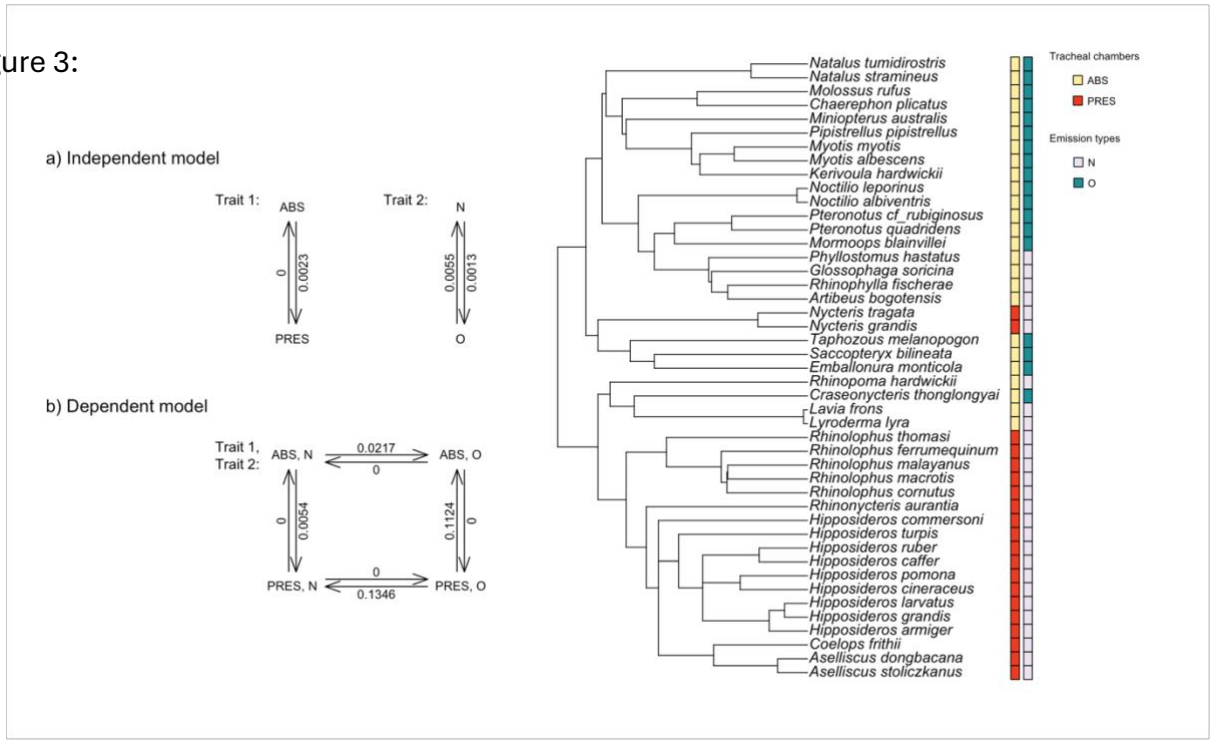

Figure 4:

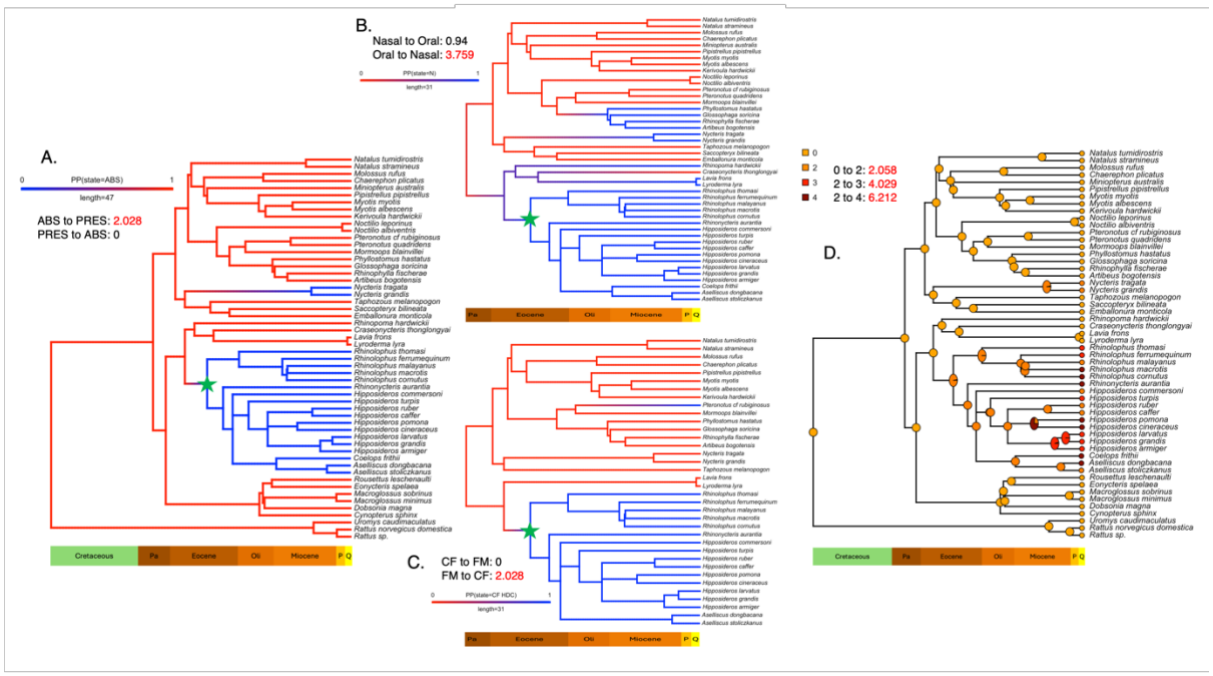

Supplementary:

Figures:

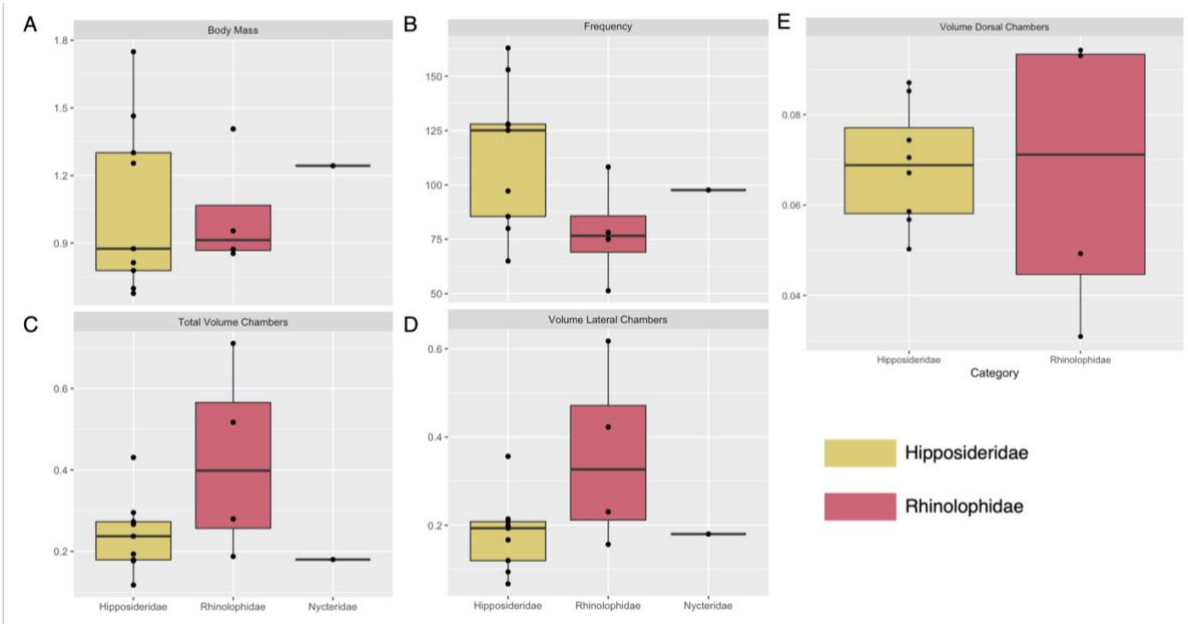

Figure S1: Distributions of body mass, frequency of maximum energy (FME), and volumes of tracheal chambers in Hipposideridae (n = 9), Rhinolophidae (n = 4), and Nycteridae (n = 1). A, Body mass; B, Frequency; C, Total volume chambers; D, Volume lateral chambers; E, Volume dorsal chambers. Related to Figure 2.

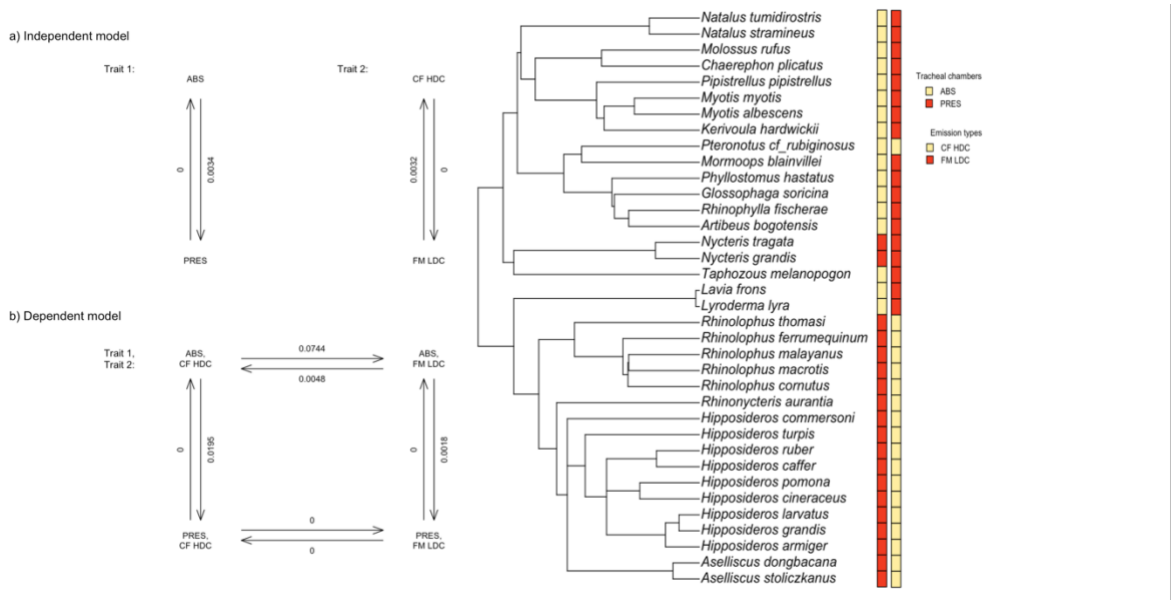

Figure S2: Different correlated evolution models of the tracheal chambers and the laryngeal echolocating behaviours. a), dependent model; b), independent model. Arrows indicate the direction and rates of transition between states. Related to Figure 3 and Table 2A.

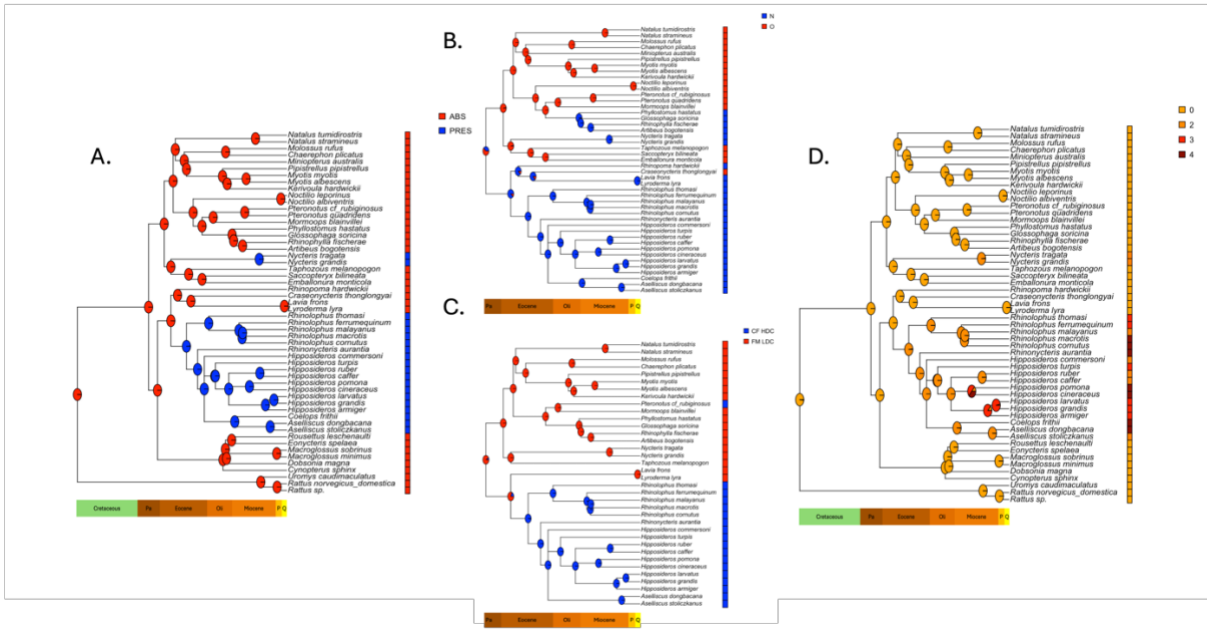

Figure S3: Marginal ancestral state reconstructions (ASR). Related to Figure 4 and Table S2. A, ASR of the tracheal chambers acquisition with Dataset 1; B, ASR of the type of emission with Dataset 3; C, ASR of the laryngeal echolocating strategies with Dataset 3; D, ASR of the diversification of tracheal chambers with Dataset 1. ABS, absence of chamber; PRES, presence of chambers; CF HDC, constant frequency and high duty cycle calls; FM LDC, frequency-modulated and low duty cycle calls; N, nasal emission; O, oral emission; Pa, Paleocene; Oli, Oligocene; P, Pliocene; Q, Quaternary.

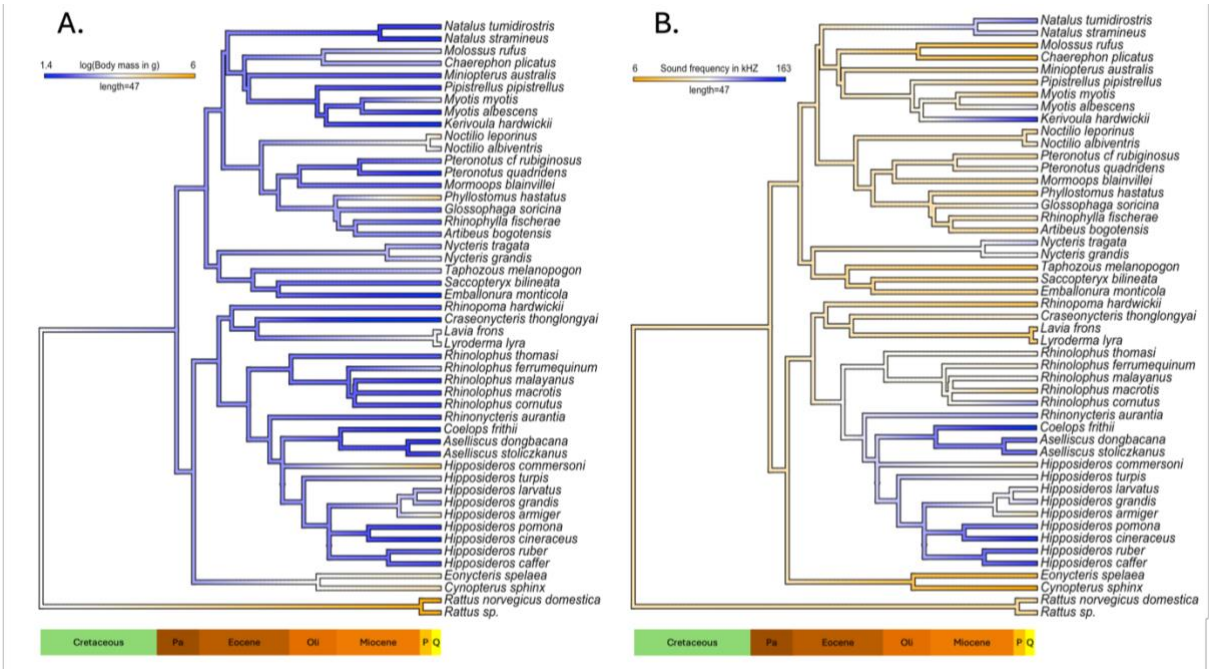

Figure S4: Ancestral state reconstruction using Brownian Motion models. Related to Figure 4 and Table S3. A. Ancestral state reconstruction of the log(e) of body mass; B, Ancestral state reconstruction of the frequency of maximum energy (FME). Pa, Paleocene; Oli, Oligocene; P, Pliocene; Q, Quaternary.

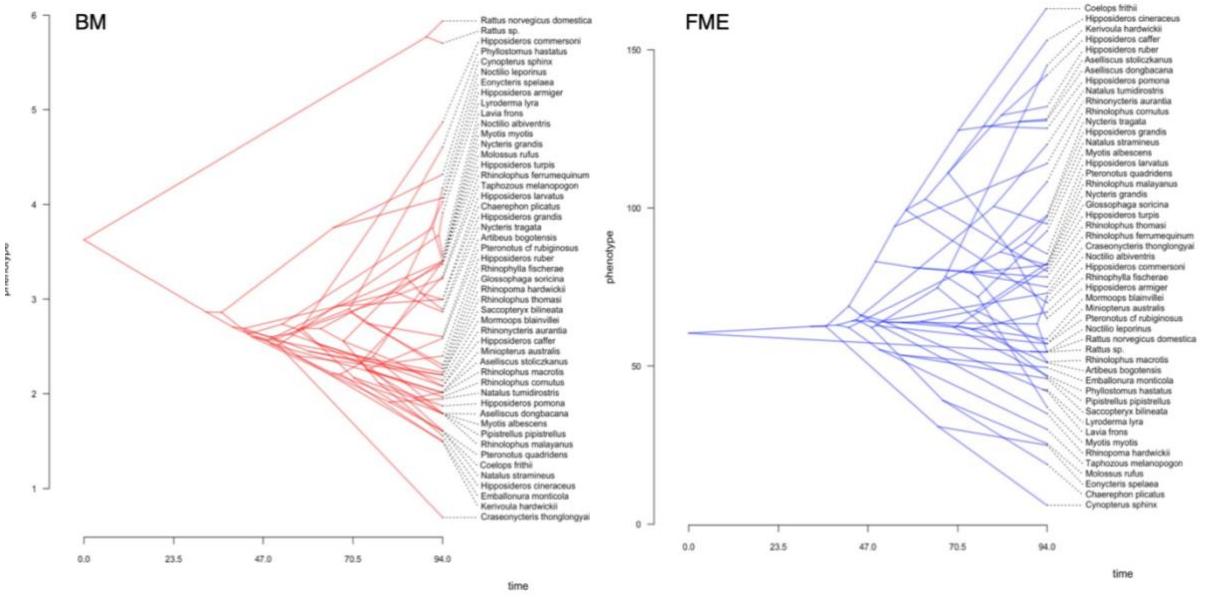

Figure S5: Evolution of the different phenotypes through time illustrating a Brownian motion distribution of the data (random evolution). Related to Figure 4. A, phenogram of the body mass

30 evolution; B, phenogram of the frequency of maximum energy (FME) evolution. The time on the
31 horizontal X-axis is in millions of years.

Tables:

Table S1: Phylogenetic independent contrasts of the frequency of maximum energy (FME), body mass (BM) and volume of tracheal chambers (VTC). Related to Figure 2.

MODEL	p-value	Estimate	R^2
FME/BM (ALL)	**$6.993e^{-05}$**	-0.25430	0.2781
FME/BM (w/ TC)	**0.01005**	-0.27125	0.3901
FME/VTC	**$2.003e^{-05}$**	-0.28154	0.7749
VTC/BM	**$4.128e^{-05}$**	1.1355	0.7467

Table S2: Comparison of the different Mk (Markov k-state) models for acquisition and diversification of the tracheal chambers. Bold values show the best model to fit the data. Related to Figure 4 and Figure S3.

Parameters	MK1	Mk2	Mk3	Mk4	MX1	MX2
AICc	71.1693	**67.6074**	74.0467	87.2687	21.3625	22.2069
Likelihood	-32.3119	**-29.3386**	-27.1772	-27.1772	-9.6378	-8.9701
Akaike weight	0.107	**0.769**	0.122	0.002	0.582	0.418

Table S3: Results of the evolutionary models to fit the data. FME, frequency of maximum energy; BM, Brownian Motion; EB, Early-burst; OU, Ornstein-Uhlenbeck. Related to Figure S4.

Variable	BM	EB	OU
FME	0.549	0.202	0.248
lnBodyMass	0.501	0.184	0.314

Table S4: Species distribution in datasets. D1 includes all species sampled. D2 includes all species for which FME values were found. D3 includes only laryngeal echolocating species. D4 only includes species that emit in CF HDC or FM LDC strategies. D5 includes species possessing tracheal chambers.

	3D Surfaces	D1	D2	D3	D4	D5
Artibeus bogotensis		✓	✓	✓	✓	
Aselliscus_dongbacana	✓	✓	✓	✓	✓	✓
Aselliscus_stoliczkanus	✓	✓	✓	✓	✓	✓
Chaerephon_plicatus		✓	✓	✓	✓	
Coelops_frithii	✓	✓	✓	✓		✓
Craseonycteris_thonglongyai		✓	✓	✓		
Cynopterus_sphinx		✓	✓			
Dobsonia_magna		✓				
Emballonura_monticola		✓	✓	✓		
Eonycteris_spelaea	✓	✓	✓			
Glossophaga_soricina		✓	✓	✓	✓	
Hipposideros_armiger	✓	✓	✓	✓	✓	✓
Hipposideros_caffer		✓	✓	✓	✓	
Hipposideros_cineraceus	✓	✓	✓	✓	✓	✓
Hipposideros_commersoni		✓	✓	✓	✓	
Hipposideros_grandis	✓	✓	✓	✓	✓	✓
Hipposideros_larvatus	✓	✓	✓	✓	✓	✓
Hipposideros_pomona	✓	✓	✓	✓	✓	✓
Hipposideros_ruber		✓	✓	✓	✓	
Hipposideros_turpis	✓	✓	✓	✓	✓	✓
Kerivoula_hardwickii		✓	✓	✓	✓	
Lavia_frons		✓	✓	✓	✓	
Lyroderma_lyra		✓	✓	✓	✓	
Macroglossus_minimus		✓				
Macroglossus_sobrinus		✓				

Miniopterus_australis		✓	✓	✓		
Molossus_rufus		✓	✓	✓	✓	
Mormoops_blainvillei		✓	✓	✓	✓	
Myotis_albescens		✓	✓	✓	✓	
Myotis_myotis		✓	✓	✓	✓	
Natalus_stramineus		✓	✓	✓	✓	
Natalus_tumidirostris		✓	✓	✓	✓	
Noctilio_albiventris		✓	✓	✓		
Noctilio_leporinus		✓	✓	✓		
Nycteris_grandis		✓	✓	✓	✓	
Nycteris_tragata	✓	✓	✓	✓	✓	✓
Phyllostomus_hastatus		✓	✓	✓	✓	
Pipistrellus_pipistrellus		✓	✓	✓	✓	
Pteronotus_cf_rubiginosus		✓	✓	✓	✓	
Pteronotus_quadridens		✓	✓	✓		
Rattus_norvegicus_domestica	✓	✓	✓			
Rattus_sp.		✓	✓			
Rhinolophus_cornutus	✓	✓	✓	✓	✓	✓
Rhinolophus_ferrumequinum	✓	✓	✓	✓	✓	✓
Rhinolophus_macrotis	✓	✓	✓	✓	✓	✓
Rhinolophus_malayanus		✓	✓	✓	✓	
Rhinolophus_thomasi	✓	✓	✓	✓	✓	✓
Rhinonycteris_aurantia	✓	✓	✓	✓	✓	✓
Rhinophylla_fischerae		✓	✓	✓	✓	
Rhinopoma_hardwickii		✓	✓	✓		
Rousettus_leschenaulti		✓				
Saccopteryx_bilineata		✓	✓	✓		
Taphozous_melanopogon		✓	✓	✓	✓	
Uromys_caudimaculatus		✓				

51

52 Table S5: Use of datasets for each analysis. FME, frequency of maximum energy; NO, type of
53 emission (nasal or oral); NTC, number of tracheal chambers; PGLS, phylogenetic generalized least
54 squares; PIC, phylogenetic independent contrasts; ST, strategies of laryngeal echolocation; TC,
55 tracheal chambers.

Tests	Dataset(s)	Tests	Dataset(s)
Boxplots	D2	Threshold model (NO)	D3
PIC (All Bats)	D2	Threshold model (ST)	D4
PIC (Bats with TC)	D5	Threshold model (FME)	D2
PGLS (All Bats)	D2	Marginal and Stochastic model (TC)	D1
PGLS (Bats with TC)	D5	Marginal and Stochastic model (NTC)	D1
MK models	D1	Marginal and Stochastic model (NO)	D3
Pagel's model (NO)	D3	Marginal and Stochastic model (ST)	D4
Pagel's model (ST)	D4	Ancestral state reconstruction	D2

56

Table S6: Species and data collected for each associated variable. CF HDC, constant frequency high duty cycle; FM LDC, frequency modulated low duty cycle; FME, frequency of maximum energy; N-O, nasal or oral emitter; TC, number of tracheal chambers. Guild names from Denzinger and Schnitzler (2013).

Species	Family	N-O	Strategy	TC	FME (kHz)	Body mass (g)	Guilds	Volume chambers total (mm3)	Volume lateral chambers (mm3)	Volume dorsal chambers (mm3)
Artibeus_bogotensis	Phyllostomidae	N	FM LDC	0	51	13.5	NSPAG	0.00E+00	0	0
Aselliscus_dongbacanus	Hipposideridae	N	CF HDC	4	127.5	6	NSFD	1.771605	1.249109	0.522496
Aselliscus_stoliczkanus	Hipposideridae	N	CF HDC	2	128	7.5	NSFD	1.450207	1.450207	0
Mops_plicatus	Molossidae	O	FM LDC	0	19	20	OSA	0.00E+00	0	0
Coelops_frithii	Hipposideridae	N	CF LDC	4	163	5	NSFD	0.586786	0.33545	0.251336
Craseonycteris_thonglongyai	Craseonycteridae	O	CF LDC	0	73	2	NSPG	0	0	0
Cynopterus_sphinx	Pteropodidae	None	None	0	6	75	None	0.00E+00	0	0
Dobsonia_magna	Pteropodidae	None	None	0	NA	475	None	0.00E+00	0	0
Emballonura_monticola	Emballonuridae	O	CF/FM LDC	0	49.5	4.5	OSA	0.00E+00	0	0
Eonycteris_spelaea	Pteropodidae	None	None	0	25	58.5	None	0.00E+00	0	0
Glossophaga_soricina	Phyllostomidae	N	FM LDC	0	81	9.6	NSPAG	0.00E+00	0	0
Hipposideros_armiger	Hipposideridae	N	CF HDC	3	65	56.1	NSFD	15.30581	12.01903	3.28678
Hipposideros_caffer	Hipposideridae	N	CF HDC	2	142	8	NSFD	0.00E+00	0	0
Hipposideros_cineraceus	Hipposideridae	N	CF HDC	4	153	4.75	NSFD	0.852476	0.447602	0.404874
Hipposideros_commersoni	Hipposideridae	N	CF HDC	2	70	130	NSFD	0.00E+00	0	0
Hipposideros_grandis	Hipposideridae	N	CF HDC	3	97.2	17.95	NSFD	4.25867	2.99269	1.26598
Hipposideros_larvatus	Hipposideridae	N	CF HDC	3	85.5	20	NSFD	5.32775	3.98498	1.34277
Hipposideros_gentilis	Hipposideridae	N	CF HDC	4	125.1	6.5	NSFD	1.148731	0.779615	0.369116
Hipposideros_ruber	Hipposideridae	N	CF HDC	2	132	11	NSFD	0.00E+00	0	0
Hipposideros_turpis	Hipposideridae	N	CF HDC	3	80	29.1	NSFD	12.53013	10.36541	2.16472
Kerivoula_hardwickii	Vespertilionidae	O	FM LDC	0	145	4.45	OSA	0.00E+00	0	0
Lavia_frons	Megadermatidae	N	FM LDC	0	42	32	NSPG	0.00E+00	0	0
Lyroderma_lyra	Megadermatidae	N	FM LDC	0	42.5	50	NSPG	0.00E+00	0	0
Macroglossus_minimus	Pteropodidae	None	None	0	NA	18	None	0.00E+00	0	0
Macroglossus_sobrinus	Pteropodidae	None	None	0	NA	20.75	None	0.00E+00	0	0

Miniopterus_australis	Miniopteridae	O	CF/FM LDC	0	57	7.5	ESA	0.00E+00	0	0
Molossus_rufus	Molossidae	O	FM LDC	0	25.5	30	OSA	0.00E+00	0	0
Mormoops_blainvillei	Mormoopidae	O	FM LDC	0	58.5	8.5	ESA	0.00E+00	0	0
Myotis_albescens	Vespertilionidae	O	FM LDC	0	92.7	6	EST	0.00E+00	0	0
Myotis_myotis	Vespertilionidae	O	FM LDC	0	37	30	EST	0.00E+00	0	0
Natalus_stramineus	Natalidae	O	FM LDC	0	95	5	NSPAG	0.00E+00	0	0
Natalus_tumidirostris	Natalidae	O	FM LDC	0	120	7	NSPAG	0.00E+00	0	0
Noctilio_albiventris	Noctilionidae	O	CF/FM LDC	0	72	30	EST	0.00E+00	0	0
Noctilio_leporinus	Noctilionidae	O	CF/FM LDC	0	54.5	65	EST	0.00E+00	0	0
Nycteris_grandis	Nycteridae	N	FM LDC	2	82	30	NSPG	0.00E+00	0	0
Nycteris_tragata	Nycteridae	N	FM LDC	2	97.64	17.5	NSPG	3.15051	3.15051	0
Phyllostomus_hastatus	Phyllostomidae	N	FM LDC	0	47	100	NSPAG	0.00E+00	0	0
Pipistrellus_pipistrellus	Vespertilionidae	O	FM LDC	0	46.5	6	OSA	0.00E+00	0	0
Pteronotus_cf_rubiginosus	Mormoopidae	O	CF HDC	0	57	13.25	NSFD	0.00E+00	0	0
Pteronotus_quadridens	Mormoopidae	O	CF LDC	0	82.5	5	ESA	0.00E+00	0	0
Rattus_norvegicus_domestica	Muridae	None	None	0	54.39	380	None	0.00E+00	0	0
Rattus_sp.	Muridae	None	None	0	54.39	300	None	0.00E+00	0	0
Rhinolophus_cornutus	Rhinolophidae	N	CF HDC	4	108.25	7.14	NSFD	1.338991	1.118204	0.220787
Rhinolophus_ferrumequinum	Rhinolophidae	N	CF HDC	3	75	25.5	NSFD	7.13307	5.87655	1.25652
Rhinolophus_macrotis	Rhinolophidae	N	CF HDC	4	51.3	7.45	NSFD	5.293002	4.59971	0.693292
Rhinolophus_malayanus	Rhinolophidae	N	CF HDC	2	82	6	NSFD	0.00E+00	0	0
Rhinolophus_thomasi	Rhinolophidae	N	CF HDC	3	78.2	9	NSFD	4.652795	3.80436	0.848435
Rhinonycteris_aurantia	Rhinonycteridae	N	CF HDC	4	114	8	NSFD	2.069959	1.41758	0.652379
Rhinophylla_fischerae	Phyllostomidae	N	FM LDC	0	67	10	NSPG	0.00E+00	0	0
Rhinopoma_hardwickii	Rhinopomatidae	N	CF/FM LDC	0	35	9.25	OSA	0.00E+00	0	0
Rousettus_leschenaulti	Pteropodidae	None	None	0	NA	82	None	0.00E+00	0	0
Saccopteryx_bilineata	Emballonuridae	O	CF/FM LDC	0	46	9	OSA	0.00E+00	0	0
Taphozous_melanopogon	Emballonuridae	O	FM LDC	0	30	25	OSA	0.00E+00	0	0
Uromys_caudimaculatus	Muridae	None	None	0	NA	650	None	0.00E+00	0	0